Research Article

Insights of Clinical and Medical Images

Resting-State Neural Network Disturbances Underlying The Subacute Stage Of Poststroke Aphasia

Xiao Wang[1+],Tao Feng[2+], Lulu Cai[1], Yingying Xia[1], Ke Yu[1], Jingyun Sha[1], Chao Zhang[1*] and Jie Xiang[2*]

[1]Department of Radiology, Affiliated Hospital of Xuzhou Medical University, Xuzhou 221000, Jiangsu, P.R. China
[2]Department of Rehabilitation, Affiliated Hospital of Xuzhou Medical University, Xuzhou 221000, Jiangsu, P.R. China
[+] All authors are contributed equally to this work

*Corresponding Author:
Chao Zhang, Jie Xiang,
Department of Radiology, Department of Rehabilitation, Affiliated Hospital of Xuzhou Medical University, Xuzhou 221000, Jiangsu, P.R. China,
Email: chaozhang0328@hotmail.com; 2625653828@qq.com.

Received Date: 30 July 2024
Accepted Date: 07 Aug 2024
Published Date: 12 Aug 2024

Citation:
Chao Zhang, Jie Xiang. Resting-State Neural Network Disturbances Underlying The Subacute Stage Of Poststroke Aphasia. Insights of Clinical and Medical Images 2024.

1. Abstract

1.1. Background: To explore the brain activity characteristics in normal parenchyma outside the stroke lesion in subacute stage of PSA by fMRI, to further explain the mechanism of language remodelling.

1.2. Methods: Patients with PSA at subacute stage aged between 31-69 years and age/sex-similar healthy controls (HCs) were recruited in this study. All patients underwent fMRI scanning and Western Aphasia Battery (WAB) measures, all HCs only underwent fMRI scanning. A dynamic approach was used to investigate the functional connectivity between networks (FNC) across all subjects. Independent component analysis was carried out to extract RSNs, and the sliding window method was used to obtain dynamic FNC (dFNC) patterns. State analysis was conducted to explore the potential alterations in FNC and other dynamic metrics.

1.3. Results: Three sets of coupling as left frontoparietal network (lFPN) with right frontoparietal network (rFPN), lFPN with posterior default mode network (pDMN), and pDMN with salience network (SN), differed between the PSA and HC groups in specific state ($p<0.05$, FDR correction). The strength of FC between the lFPN and rFPN was positively correlated with yes/no questions and sequential commands ($p=0.737$, $r=0.023$ and $p=0.021$, $r=0.745$, respectively).

1.4. Conclusions: Abnormal coupling of brain activities was revealed in normal brain parenchyma outside stroke lesions. The aberrant FNC patterns were state-dependent in PSA. Reduced lFPN-rFPN connectivity may be the key element involved in auditory verbal comprehension. Overall, these findings has extended our understanding of the underlying pathophysiological mechanisms of PSA.

2. Keywords:
Resting-state, Stroke, Aphasia, Dynamic, Functional connectivity

3. Introduction

The existing research on poststroke aphasia (PSA) based on resting-state fMRI (rs-fMRI) suggests that widespread cerebral regions are involved in addition to stroke lesions [1-4]. With brain reperfusion around the stroke focus and the disappearance of peripheral inflammation in the subacute stage of PSA, the remodelling of language functions depends mainly on the compensation of normal tissue beside the stroke foci [5-8]. Understanding how functional organization interacts in normal tissue is essential for clinical rehabilitation. However, this issue has not yet been elucidated. In this regard, it is necessary to develop new methods for investigating the neurobiological mechanisms underlying subacute PSA. Functional connectivity (FC) is considered a robust method for noninvasively measuring spontaneous brain activity [4,9]. Rs-FC studies of static functional connectivity between networks (FNC) have made great contributions regarding the neurobiological foundations of language-related disorders. For example, the left frontoparietal network (lFPN) has been shown to have decreased FNC in multiple areas of the brain in patients suffering from PSA [10]. In another study, it was found that the key factor leading to degenerative apraxia was the destruction of FNC in the supplementary motor area [11]. However, such approaches have failed to address the time-varying properties of spontaneous brain activity in the human brain. Recently, dynamic FNC (dFNC), which assumes that the FNC evolves over time, has been used to capture the fluctuating states of connectivity across the time domain [12].

In recent studies, dFNC has attracted much interest in investigations of the mechanical properties of the human brain with high replication. For example, Liu et al. [9] observed state-specific dFNC disruptions in the default mode network (DMN) in epilepsy, and these disruptions can be used to identify epilepsy patients from controls with high accuracy. Stefaniak et al. 8 revealed a different dFNC pattern between adolescent girls with and without emotional symptoms, which is potentially valuable

for the early diagnosis and specific intervention of this disorder. It was also [13] found that Parkinson's disease (PD) patients presented abnormal temporal property changes in the dFNC. These investigations indicated that assessing dFNC is important for detecting abnormal brain connections. To date, little attention has been given to the role of dFNC in the exploration of the brain network connections of patients with subacute PSA. Therefore, our objective was to explore the potential neural mechanisms of PSA. We hypothesized that dFNC would show significant variation in patients with PSA, which would be meaningfully linked to clinical manifestations. Overall, this study may provide new insight into the underlying pathophysiological mechanisms and a potential direction for therapeutic research.

4. Materials and Methods

4.1. Subjects

We recruited patients with PSA at the subacute stage aged between 31 and 69 years who were hospitalized in the Department of Rehabilitation from June 2019 to June 2021. All patients underwent Western Aphasia Battery (WAB) testing14 and MRI scanning one month after stroke. Patients were enrolled based on the following criteria: (i) left cerebral hemisphere stroke; (ii) persistent aphasia occurring 24 hours after stroke; (iii) age ≥18 years; (iv) right-handed; (v) no other lesions, such as tumour and vascular malformation, in the brain. The exclusion criteria were as follows: (i) MRI revealing other intracranial lesions in addition to stroke foci; (ii) history of mental disorders or taking drugs that may affect the nervous system within last year; and (iii) inability to complete the MRI scan. Age- and sex-matched volunteers were enrolled as the healthy controls (HCs). As a primary inclusion criterion, the HCs had to meet the following conditions: (i) match patients with PSA in terms of age and sex; (ii) no mental or nervous system disorders; (iii) no use of any drugs within the last year that could have affected the nervous system; and (v) right-handedness. The following criteria were used to exclude candidates: (i) routine MRI scans revealing intracranial lesions; (ii) neurological disorders; and (iii) drug or alcohol abuse. Finally, 20 patients (11 males and 9 females, age: 46.5±11.9 years) and 20 HCs (13 males and 7 females, age: 45.3±13.5 years) were included for analysis.

4.2. Acquisition of MRI data

All participants underwent MRI scans with a 3.0 T MRI (Signa HD; GE Medical Systems, Waukesha, WI, USA). For noise reduction, each subject wore appropriate earplugs during scanning. We acquired T1-weighted images (T1WIs) with 1 mm isotropic voxels and 192 slices using a 3D-T1 BRAVO sequence (typical repetition time (TR) and echo time (TE) were 7 seconds and 3 seconds, respectively, the flip angle was 12°, and the field of view (FOV) was 256 mm × 256 mm). An echo-planar imaging sequence was carried out to obtain rs-fMRI raw data with 36 slices and 185 volumes, and the parameters were as follows: TR/TE, 2000 ms/30 ms; FOV, 220 mm × 220 mm; voxel size, 3.4 mm × 3.4 mm × 4.0 mm; and flip angle, 90°.

4.3. Lesion delineation

Stroke lesion delineation and volume calculation were processed by ITK-SNAP software (http://www.itksnap.org) (Figure 1). Two radiologists with at least two years of experience in neuroradiology delineated the lesions on T1WI. Each patient's final result was the average of each volume obtained by each radiologist. If there was any dispute about volume delineation, it was reviewed with a high-level doctor to maintain the consistency of the description.

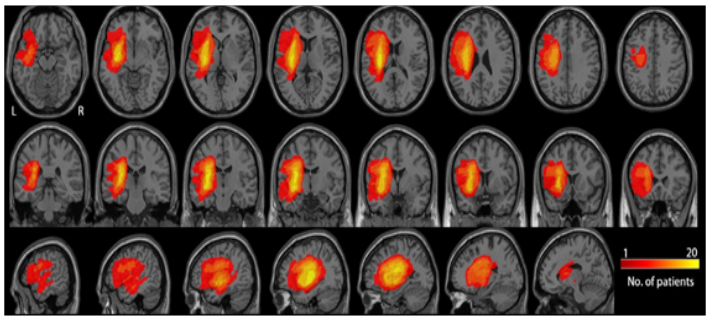

Figure 1: Distribution of each individual lesion for all patients with PSA. The lesion area overlap across patients was rendered on the brain. Colours represent the number of lesions in each patient to a specific voxel. L represents left and R represents right.

4.4. Preprocessing of rs-fMRI Data

Raw data preprocessing was performed using the graph theoretical network analysis toolbox for imaging connectomics (GRETNA) (https://www.nitrc.org/projects/gretna/) 15. The first step was to remove the first 10 time points for each subject. Then, time differences were corrected for each subject through slice timing. Afterwards, a Friston-24 model was applied to correct head motion in the realigning step, and any results were excluded from the analysis if the maximum displacement of the head was greater than 2 mm, the maximum rotation was more than 2.0°, or the mean framewise displacement exceeded 0.3 [16, 17]. Subsequently, normalization of the patients and HCs was carried out separately. By using the 'clinical toolbox' of Parametric Mapping version 12 (http://www.fil.ion.ucl.ac.uk/spm/), individual structural images of PSA patients were segmented and normalized to Montreal Neurological Institute (MNI) space. To avoid bias during spatial normalization, the clinical toolbox utilizes a cost function modification that excludes the lesion area [18]. Transformation parameters were used to normalize functional imaging data to MNI space and resample to 3 mm × 3 mm × 3 mm. HC data were morphed into MNI atlas space using diffeomorphic anatomical registration through exponentiated lie algebra (DARTEL) normalization [19,20]. Finally, all functional volumes were smoothed spatially using a Gaussian kernel with a full-width-at-half-maximum of 6 mm.

4.5. Independent component analysis

Group ICA of fMRI Toolbox (GIFT) software was employed to carry out independent component analysis (ICA) [21]. The following steps were as follows: (i) data reduction; (ii) automatic estimation of

independent components (ICs); (iii) group analysis of ICA; and (iv) back reconstruction for each component at the individual level [22]. We conducted a one-sample t test with random effects to estimate each IC for all the participants' maps (family error correction, $p<0.05$, voxel threshold >50) by using SPM12 software [23].

4.6. Dynamic FNC

For this step, a temporal dFNC toolbox within the GIFT software was used. Before dynamic FNC calculation, all time courses of the selected ICs were bandpass filtered (0.01–0.08 Hz) and detrended to reduce the influence of physiological noise and scanner drifting, and simultaneous time course despiking was performed to reduce the impact of movement 'spikes' [9, 24, 25]. Briefly, the process of despiking includes detecting spikes as determined by the 3d-Despike algorithm and replacing spikes by the value obtained from third-order spline fit to neighbouring clean portions of the data [25]. Then, dFNC was calculated using a sliding window technique. According to previous research, the best estimated dFNC window width is between 30 and 60 seconds (Liégeois R et al., 2016). The chosen window length of 60 s (2 s×30) has been suggested to be suitable for capturing dynamics in FNC [26, 27]. In this study, we selected a window length of 60 s for the dFNC process, and the window segment was tapered by convolving a rectangle (width 30, TRs=60 s) with a Gaussian distribution (σ=3 TRs) and advancing 1 TR at each step [28]. Finally, the covariance matrices for each window were concatenated to form a component × component × window array to represent the changes in covariance between networks as a function of time [24]. Five clusters were derived from 150 replicate dFNC windows using clustering of k-means with the squared Euclidean distance and 500 iterations [29]. Using the elbow criterion, the best centroid state number was determined [9, 24] and a k of 5 was determined (Figure 2). As a final step, all data were then grouped into 5 clusters using the cluster centroids as starting points, and FC states were determined by cluster medians.

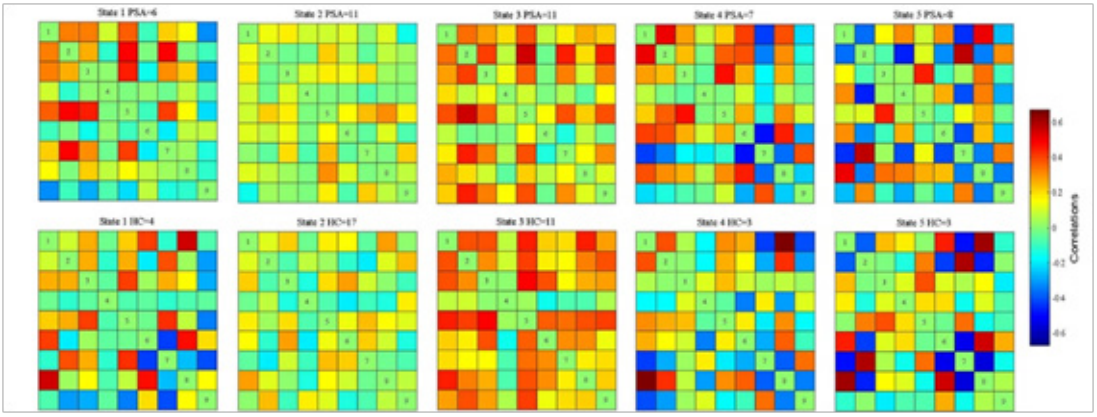

Figure 2: The five clusters of all subjects. Group-specific centroids of the states for patients with PSA and healthy controls together with the count of subjects in each state, respectively. The colour bar represents the z value of the FNC. Abbreviations: PSA, poststroke patient.

4.7. Statistical Analysis

The Kolmogorov–Smirnov test (K-S) was employed to test whether the data of continuous variables obeyed a normal distribution. The data that conformed to a normal distribution were tested by a two-sample t test. In the case of a nonnormal distribution, a nonparametric test was used. The chi-square test was used to assess the sex difference between the two groups. Multiple comparisons (FDR correction) were used to measure the intergroup differences in dFNC and three temporal metrics. The three temporal metrics included mean dwell time, fraction time and the total number of state transitions. To observe whether the statistically significant results above have a significant correlation with WAB tests, we employed Pearson correlation to observe the correlation between dFNC and WAB scores as well as between temporal metrics/lesion volume and WAB scores. The above statistical thresholds were all set toP less than 0.05.

5. Results

5.1. Subjects

Finally, 20 patients (11 males and 9 females, age: 46.5±11.9 years) and 20 HCs (13 males and 7 females, age: 45.3±13.5 years) were included for analysis. The following table lists the demographic data, lesion volume and clinical data of all subjects (Table 1). The data of continuous variables conform to a normal distribution by K-S assessment. There was no significant difference in age ($p=0.740$) or sex ($p=0.748$) between the groups. The delineation of lesion volume was highly consistent between the two radiologists (weighted $\kappa = 0.80$).

Insights of Clinical and Medical Images

Table 1: Characteristics of each patient with PSA

Patients	Gender	Age	Lesion (cm3)	Yes/no questions	Word recognition	Sequential commands	Repetition	Object naming	Word fluency	Sentence completion	Responsive speech	Information content	Fluency
P003	M	47	28.32	48	42	45	70	20	1	7	6	5	4
P004	M	43	21.11	45	40	42	66	34	8	8	9	9	6
P005	M	46	43.32	56	36	36	67	30	6	9	7	9	5
P006	F	69	24.82	50	51	66	68	29	3	5	8	5	6
P008	F	32	57.03	56	45	65	53	43	1	4	4	3	5
P009	F	51	43.35	46	38	55	61	28	1	2	1	2	6
P010	F	54	24.76	45	37	21	62	13	0	6	2	2	8
P011	M	38	51.52	52	55	50	65	25	0	7	5	4	4
P012	F	50	42.9	45	52	48	68	33	5	3	2	3	6
P013	M	31	25.69	51	39	22	60	36	2	6	4	9	7
P014	M	66	50.35	49	50	52	67	20	0	3	1	6	5
P015	M	47	17.31	52	48	35	60	12	0	2	5	4	5
P018	M	33	42.91	57	37	48	72	17	6	4	8	4	8
P019	M	62	8.98	58	56	45	63	26	2	8	9	4	6
P020	F	65	7.41	56	52	40	66	24	0	3	5	3	7
P021	M	50	25.33	42	40	42	75	30	3	6	7	6	8
P022	F	33	32.05	48	58	75	99	48	1	8	10	9	9
P023	F	43	28.37	52	55	45	61	32	2	10	2	1	5
P024	M	39	21.12	50	38	53	60	12	0	4	4	4	5
P025	F	34	43.36	46	36	42	65	19	2	7	10	7	8

5.2. Networks of Interest

Nine ICs representing the typical RSN were identified from 23 ICs, representing the typical RSN (Figure 3): IC 02 (medial visual network, mVN); IC 04 (sensorimotor network, SMN); IC 06 (posterior default mode network, pDMN); IC 07 (anterior insular cortex of salience network, named SN1); IC 08 (visuospatial network, VisN); IC 09 (left frontoparietal network, lFPN); IC 10 (right frontoparietal network, rFPN); IC 17 (lateral visual network, lVN); and IC 20 (anterior cingulate cortex of salience network, named SN2).

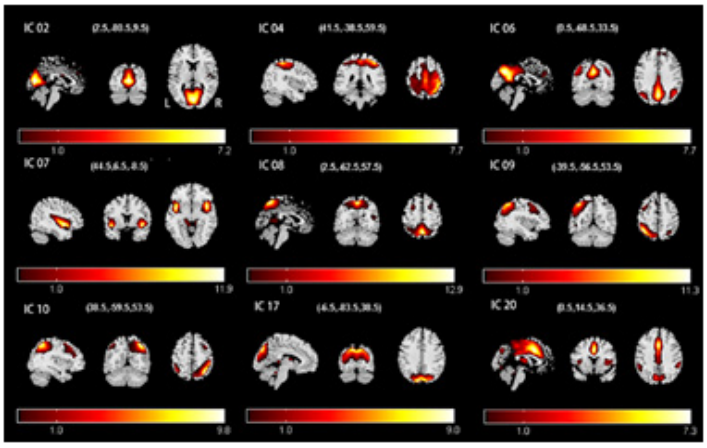

Figure 3: Nine independent components (ICs) of our interest networks were displayed in spatial maps using the three most informative slices. MNI coordinates represent the most significant voxel. L represents left and R represents right.

The comparison results of dFNC between PSA and HC groupsSignificant intergroup dFNC differences were found in state 2 and state 3. Three sets of couplings (lFPN with pDMN and rFPN, pDMN with SN) differed between the PSA and HC groups. The PSA patients showed significantly higher FC between the pDMNs and SNs and lower FC between the lFPN and rFPN in state 2 than the HCs. FC between the lFPN and pDMN decreased in state 3 ($p<0.05$, FDR correction) (Figures 4b and c).

Figure 4: Significant dFNC differences between patients with PSA and HCs (B and C). The red lines represent significantly increased FNC, and the blue lines denote significantly decreased FNC in patients with PSA, compared to that in HCs. The strength of FC between the lFPN and rFPN was positively correlated with yes/no questions and Sequential commands ($p=0.737$, $r=0.023$ and $p=0.021$, $r=0.745$, respectively) (A). The orange triangle represents sequential commands, and the blue dot denotes yes/no questions. Abbreviations: dFNC, dynamic functional connectivity between networks; PSA, poststroke aphasia; HCs, healthy controls, mVN, medial visual network; SMN, sensorimotor network; pDMN, posterior default mode network; SN, salience network; VisN, visuospatial network; lFPN, left frontoparietal network; rFPN, right frontoparietal network; lVN, lateral visual network; FC, functional connectivity; WAB, Western Aphasia Battery.

Insights of Clinical and Medical Images

Figures 4a, b and c:

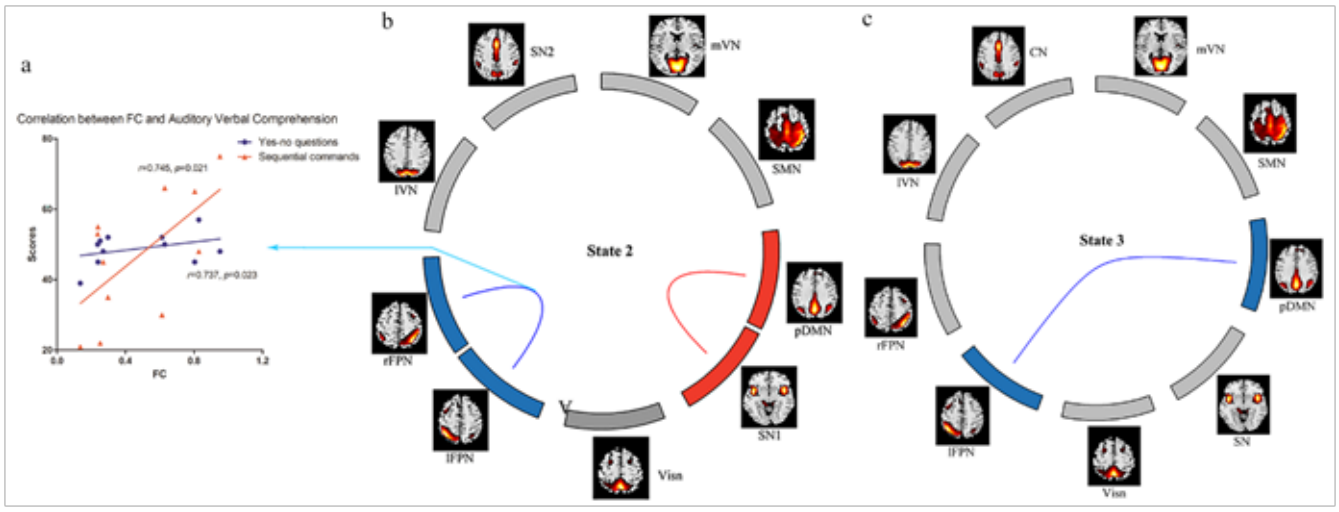

The mean dwell time in state 2 was markedly lower in the patient group than in the HC group ($p<0.05$) (Figure 5). No significant differences were found among other metrics.

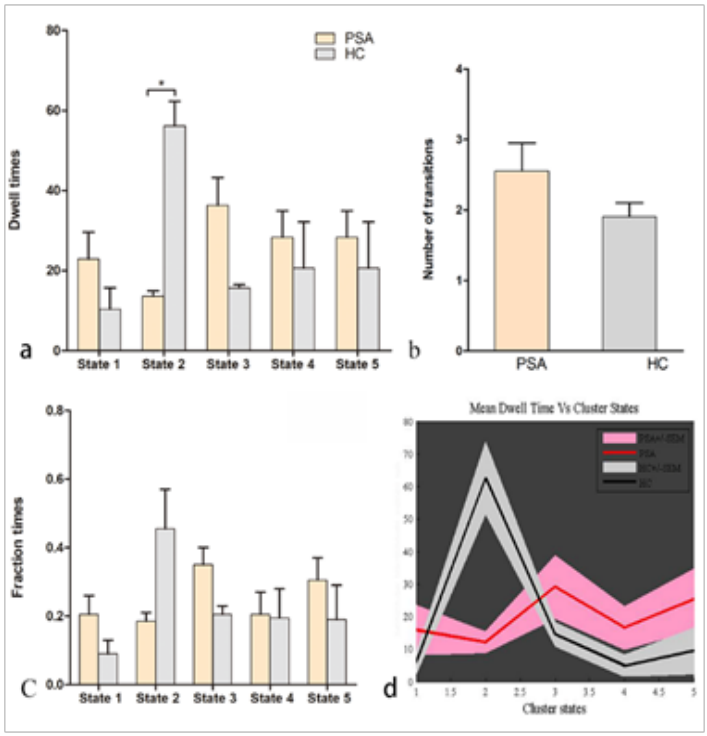

Figure 5: Intergroup comparison in temporal metrics of each state. The black stars in bar plots represent significant intergroup differences, and error bars represent the standard error (A-C). The mean dwell time in state 2 of the patient group was also significantly lower than that of the HC group (D). Abbreviations: PSA, poststroke aphasia; HCs, healthy controls.

5.3. Correlation analysis between FC and WAB scores

A Pearson correlation analysis found a significant positive correlation between FC (lFPN with rFPN) and auditory verbal comprehension (yes/no questions and sequential commands) ($p=0.023$, $r=0.737$ and $p=0.021$, $r=0.745$, respectively) (Figure 4a).

5.4. Reproducibility Data Analysis

To confirm the repeatability of the results in our research, we selected a window length of 40 s (2 s×20) to verify the stability of the dynamic analysis. The subsequent data postprocessing protocol and statistical methods remained the same. We obtained the following results when comparing patients with HCs: i) there was a significant reduction in mean dwell time in state 2 of the patient group ($p<0.05$); ii) PSA subjects showed reduced FC between the lFPN and the pDMN and between the lFPN and the rFPN ($p<0.05$, FDR correction) (Supplementary Materials and Figure S1 and S2). Intergroup differences in FC (between the lFPN and rFPN) showed a significant positive correlation with auditory verbal comprehension (yes/no questions and sequential commands) according to Pearson correlation analysis ($p = 0.038$, $r= 0.629$ and $p=0.013$, $r = 0.719$, respectively).

Figure S1: The five cluster of all subjects were also obtained via window length of 40 s (2 s×20). Group-specific centroids of the states for patientswith PSA and healthy controls together with the count of subjects in each state, respectively. The color bar represents the z value of FNC.

Insights of Clinical and Medical Images

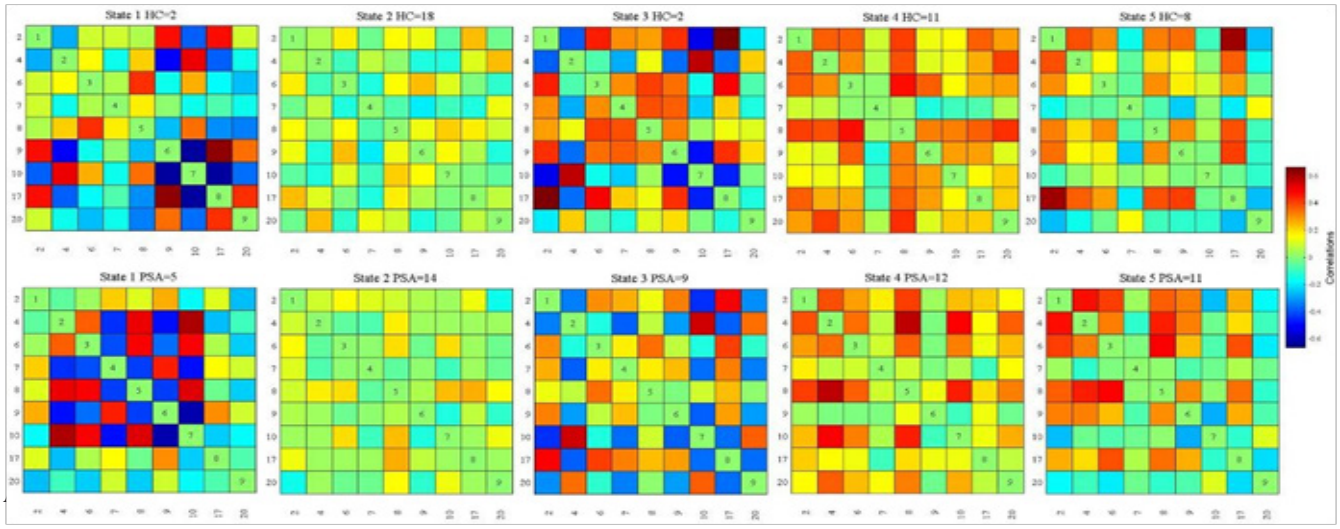

Figure S2: Inter-group comparison in temporal metrics of each state (the window length of 40 s). Mean dwell time in state 2 of the patient group was also significantly lower than that of the HCs group (A). Compared with HCs, patients showed significant decreased coupling between lFPN (9) and pDMN (6), as well as between lFPN (9) and rFPN(10) in state 4. Abbreviations: lFPN, left frontoparietal network; pDMN, posterior default mode network; SN, salience network; PSA, post-stroke aphasia;HCs,

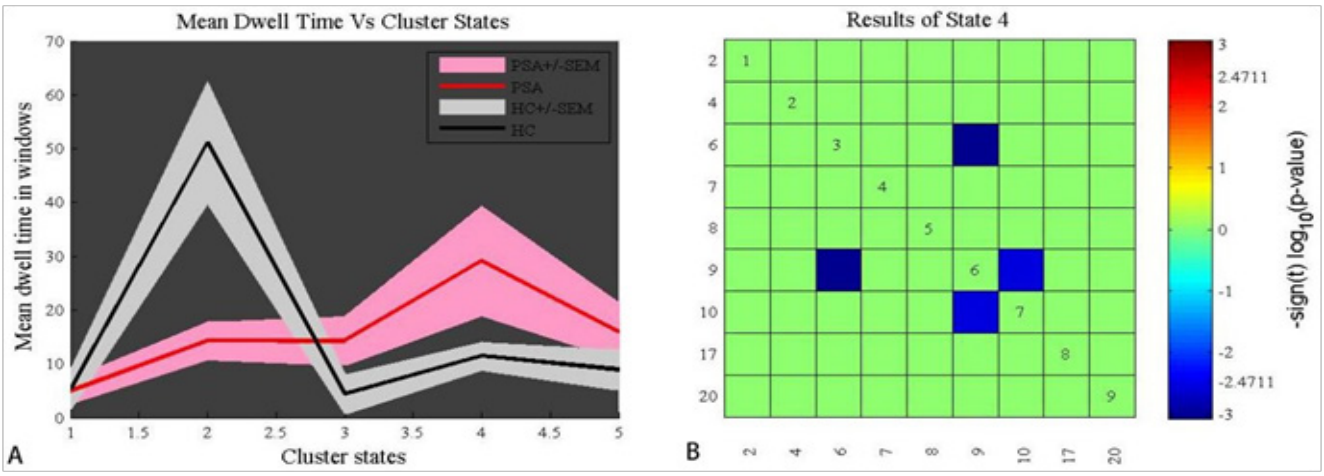

By performing sliding window dFNC analysis on rs-fMRI of patients with subacute PSA, the current investigation found that i) there were substantial alterations in dFNC, involving the pDMN, SN, and bilateral FPN, between PSA patients and HCs in specific states; ii) auditory verbal comprehension was significantly correlated with decreased FC between the lFPN and rFPN; and iii) dynamic metrics were significantly different between PSA patients and HCs. One interesting finding was that the brain connection between the lFPN and rFPN was disrupted. This also means that FC was damaged between bilateral cerebral hemispheres within the FPN, which consists of the lFPN and rFPN. Broca's area and Wernicke's area of lFPN are important language functional areas in human beings [30]. The IC representing lFPN identified in this research broadly includes these two regions. In this study, no decrease in FC associated with rFPN was found. Perhaps this is because the stroke foci were in the left cerebral hemisphere, where most of the lFPN area is located, while the right cerebral hemisphere or rFPN was not affected by stroke lesions. Our findings were similar to those of Zhu et al. 10, who found reduced FC between the lFPN and multiple cortices of the right cerebral hemisphere in PSA patients using static FC, but there were also differences in that we revealed impaired FC between the bilateral FPN. This discrepancy could be attributed to the fact that a more consistent time point (1 month after stroke) was assessed in all the patients in our study, and the dFNC reflected the connection in a specific state rather than in static FC, ignoring the impact of time-shifting properties. Additionally, auditory verbal comprehension measurements were revealed to have a positive correlation with decreased FC between the lFPN and rFPN. The result could be explained by the fact that the bilateral cerebral hemisphere disconnection caused by stroke lesions has a strong correlation with PSA. dynamic metrics were significantly different between PSA patients and HCs. One interesting finding was that the brain connection between the lFPN and rFPN was disrupted. This also means that FC was damaged between bilateral cerebral hemispheres within the FPN, which consists of the lFPN and rFPN.

Broca's area and Wernicke's area of lFPN are important language functional areas in human beings [30]. The IC representing lFPN identified in this research broadly includes these two regions. In this study, no decrease in FC associated with rFPN was found. Perhaps this is because the stroke foci were in the left cerebral hemisphere, where most of the lFPN area is located, while the right cerebral hemisphere or rFPN was not affected by stroke lesions. Our findings were similar to those of Zhu et al. 10, who found reduced FC between the lFPN and multiple cortices of the right cerebral hemisphere in PSA patients using static FC, but there were also differences in that we revealed impaired FC between the bilateral FPN. This discrepancy could be attributed to the fact that a more consistent time point (1 month after stroke) was assessed in all the patients in our study, and the dFNC reflected the connection in a specific state rather than in static FC, ignoring the impact of time-shifting properties. Additionally, auditory verbal comprehension measurements were revealed to have a positive correlation with decreased FC between the lFPN and rFPN. The result could be explained by the fact that the bilateral cerebral hemisphere disconnection caused by stroke lesions has a strong correlation with PSA. Another finding of the current study was the abnormal internetwork connections that appeared in state 2 (decreased FNC between lFPN and pDMN) and state 3 (increased connectivity between SN1 and pDMN). The DMN refers to the normal adult human brain's baseline state and includes a group of brain regions in the parietal lobe, temporal lobe and frontal cortex. These areas usually show a decrease in activity in tasks requiring concentration but an increase in activity in various forms of complex cognition [31, 32]. Similar to previous studies, the pDMN was further separated from the DMN in our research, including the praecuneus and bilateral angular gyrus [23,33]. A reduced disconnection between the lFPN and pDMN was revealed in the PSA groups when compared with the that in the HC group.

The pDMN is a cerebral cortex with high metabolic activity that has been shown to have a tight connection with the FPN in language processing [34, 35]. Therefore, the decrease in FNC between the lFPN and pDMN in this study corroborates these earlier findings. There is a triple network model of aberrant saliency mapping in psychopathology that consists of the DMN, the FPN, and the SN [36]. Many disorders, such as autism and cognitive impairment, have been reported to involve this model [36, 37]. By switching between the DMN and FPN, the SN allows the shift from self-referential to external attention, i.e., goal-directed behaviour. [38, 39]. As a result of current research, abnormal FNC of the pDMN/lFPN and pDMN/SN may indicate regulation impairment in the triple network in PSA patients. Nevertheless, the WAB score and the triple network FC have not been significantly correlated thus far. The reason for this is not clear, but it may be related to language disruption in PSA patients. Additionally, we compared the dynamic metrics between PSA and HCs. The mean dwell time and fraction time decreased in state 2 in PSA patients, and only the mean dwell time difference was significantly reduced. In addition, the total number of transitions was greater in PSA patients. These dynamic parameters can also be used as a proxy for brain network studies [9]. However, the pathophysiological significance of these dynamic parameters needs further research to confirm. These findings may be somewhat limited by the following factors. First, all the patients received treatment for stroke, and the potential impact on the study cannot be ruled out entirely. Second, this study is a data-driven analysis, and a large sample and longitudinal design are still needed to explore the mechanism of PSA. Third, we did not include PSA patients except in the subacute stage, so we should investigate PSA patients in different periods in future. Finally, the FNC has a relatively large spatial range, so it is difficult to contribute to precise therapy (for example, transcranial magnetic stimulation target therapy). In the future, more detailed and in-depth research is needed to help in the transformation of clinical therapy.

7. Conclusion

This study used dFNC analysis to investigate patients with PSA in the subacute stage. One of the most important findings of this study is that reduced lFPN-rFPN connectivity may be the key element participating in auditory verbal comprehension. There has also been evidence of an effect on the triple network model in PSA patients. Based on these findings, PSA may be caused by focal lesions in the brain network. The analysis of dFNC in PSA patients undertaken here has extended our knowledge of the underlying pathophysiological mechanisms of this disease.

8. Acknowledgements

The authors thank the patients who participated in this study and the staff of the Department of Radiology.

9. Funding

This research was supported by the Research Project of Elderly Health in Jiangsu Province (No. LKM2023014) and Hospital-level Project of Affiliated Hospital of Xuzhou Medical University (No. 2020KA013).

References

1. Brownsett SL, Warren JE, Geranmayeh F, et al. Cognitive control and its impact on recovery from aphasic stroke. Brain. 2014; 137: 242–254. DOI: 10.1093/brain/awt289.
2. Balaev V, Petrushevsky A and Martynova O. Changes in functional connectivity of default mode network with auditory and right frontoparietal networks in poststroke aphasia. Brain Connectivity. 2016; 6: 714–723. DOI: 10.1089/brain.2016.0419.
3. Fox MD. Mapping symptoms to brain networks with the human connectome. The New England journal of medicine. 2018; 379: 2237–2245. DOI: 10.1056/NEJMra1706158.
4. Klingbeil J, Wawrzyniak M, Stockert A, et al. Resting-state functional connectivity: an emerging method for the study of language networks in post-stroke aphasia. Brain and Cognition. 2019; 131: 22–33. DOI: 10.1016/j.bandc.2017.08.005.
5. Boyd LA, Hayward KS, Ward NS, et al. Biomarkers of stroke recovery:

consensus-based core recommendations from the stroke recovery and rehabilitation roundtable. Neurorehabilitation and Neural Repair. 2017; 31: 864–876. DOI: 10.1177/1545968317732680.

6. Fu Y, Liu Q, Anrather J, et al. Immune interventions in stroke. Nature Reviews. 2015; 11: 524–535. DOI: 10.1038/nrneurol.2015.144.
7. Stockert A, Wawrzyniak M, Klingbeil J,et al. Dynamics of language reorganization after left temporo-parietal and frontal stroke. Brain 2020; 143: 844–861. DOI: 10.1093/brain/awaa023.
8. Stefaniak JD, Halai AD and Lambon Ralph MA. The neural and neurocomputational bases of recovery from post-stroke aphasia. Nature Reviews 2020; 16: 43–55. DOI: 10.1038/s41582-019-0282-1.
9. Liu F, Wang Y, Li M, et al. Dynamic functional network connectivity in idiopathic generalized epilepsy with generalized tonic-clonic seizure. Human brain mapping 2017;38:957–973. DOI: 10.1002/hbm.23430.
10. Zhu D, Chang J, Freeman S, et al. Changes of functional connectivity in the left frontoparietal network following aphasic stroke. Frontiers in Behavioral Neuroscience 2014; 8: 167. DOI: 10.3389/fnbeh.2014.00167.
11. Botha H, Utianski RL, Whitwell JL, et al. Disrupted functional connectivity in primary progressive apraxia of speech. NeuroImage Clinical 2018; 18: 617–629. DOI: 10.1016/j.nicl.2018.02.036.
12. Chang C and Glover G. Time-frequency dynamics of resting-state brain connectivity measured with fMRI. NeuroImage 2010; 50: 81–98. DOI: 10.1016/j.neuroimage.2009.12.011.
13. Fiorenzato E, Strafella A, Kim J, et al. Dynamic functional connectivity changes associated with dementia in Parkinson's disease. Brain 2019; 142: 2860–2872. DOI: 10.1093/brain/awz192.
14. Shewan CM and Kertesz A. Reliability and validity characteristics of the Western Aphasia Battery (WAB). J Speech Hear Disord 1980; 45: 308-324. DOI: 10.1044/jshd.4503.308.
15. Wang J, Wang X, Xia M, et al. GRETNA: a graph theoretical network analysis toolbox for imaging connectomics. Frontiers in Human Neuroscience 2015; 9: 386. DOI: 10.3389/fnhum.2015.00386.
16. 16. Yan CG, Cheung B, Kelly C, et al. A comprehensive assessment of regional variation in the impact of head micromovements on functional connectomics. Neuroimage 2013; 76: 183–201.
17. Zhang C, Dou B, Wang J, et al. Dynamic alterations of spontaneous neural activity in Parkinson's disease: a resting-state fMRI study. Frontiers in neurology 2019; 10: 1052. DOI: 10.3389/fneur.2019.01052.
18. Brett M, Leff A, Rorden C, et al. Spatial normalization of brain images with focal lesions using cost function masking. NeuroImage, 2001; 14: 486–500. DOI: 10.1006/nimg.2001.0845.
19. Xue K, Liang S, Yang B, et al. Local dynamic spontaneous brain activity changes in first-episode, treatment-naïve patients with major depressive disorder and their associated gene expression profiles. Psychological Medicine. 2020; 30: 1–10. DOI: 10.1017/s0033291720003876.
20. Ashburner J. A fast diffeomorphic image registration algorithm. NeuroImage 2007; 38: 95–113. DOI: 10.1016/j.neuroimage.2007.07.007.
21. Calhoun V, Adali T, Pearlson G, et al. A method for making group inferences from functional MRI data using independent component analysis. Human brain mapping, 2001; 14: 140–151. DOI: 10.1002/hbm.1048.
22. Erhardt E, Rachakonda S, Bedrick E, et al. Comparison of multi-subject ICA methods for analysis of fMRI data. Human brain mapping, 2011; 32: 2075–2095. DOI: 10.1002/hbm.21170.
23. Zhang C, Yang H, Qin W, et al. Characteristics of resting-state functional connectivity in intractable unilateral temporal lobe epilepsy patients with impaired executive control function. Frontiers in Human Neuroscience 2017; 11: 609. DOI: 10.3389/fnhum.2017.00609.
24. Malhi GS, Das P, Outhred T, et al. Resting-state neural network disturbances that underpin the emergence of emotional symptoms in adolescent girls: resting-state fMRI study. The British Journal of Psychiatry 2019; 215: 545–551. DOI: 10.1192/bjp.2019.10.
25. Damaraju E, Allen EA, Belger A, et al. Dynamic functional connectivity analysis reveals transient states of dysconnectivity in schizophrenia. Neuroimage Clin 2014; 5: 298-308. 2014/08/28. DOI: 10.1016/j.nicl.2014.07.003.
26. Duncan ES and Small SL. Changes in dynamic resting state network connectivity following aphasia therapy. Brain Imaging and Behavior 2018; 12: 1141–1149. DOI: 10.1007/s11682-017-9771-2.
27. Preti MG, Bolton TA and Van De Ville D. The dynamic functional connectome: state-of-the-art and perspectives. NeuroImage 2017; 160: 41–54. DOI: 10.1016/j.neuroimage.2016.12.061.
28. Du Y, Pearlson G, Yu Q, et al. Interaction among subsystems within default mode network diminished in schizophrenia patients: a dynamic connectivity approach. Schizophrenia Research 2016; 170: 55–65. DOI: 10.1016/j.schres.2015.11.021.
29. Calhoun VD, Miller R, Pearlson G, et al. The chronnectome: time-varying connectivity networks as the next frontier in fMRI data discovery. Neuron 2014; 84: 262–274. DOI: 10.1016/j.neuron.2014.10.015.
30. Harding IH, Yücel M, Harrison BJ, et al. Effective connectivity within the frontoparietal control network differentiates cognitive control and working memory. NeuroImage 2015; 106: 144–153.
31. Raichle ME, MacLeod AM, Snyder AZ, et al. A default mode of brain function. Proceedings of the National Academy of Sciences of the United States of America 2001; 98: 676–682. DOI: 10.1073/pnas.98.2.676.
32. Broyd SJ, Demanuele C, Debener S, et al. Default-mode brain dysfunction in mental disorders: a systematic review. Neuroscience and Biobehavioral Reviews 2009; 33: 279–296. DOI: 10.1016/j.neubiorev.2008.09.002.
33. Wang C, Qin W, Zhang J, et al. Altered functional organization within and between resting-state networks in chronic subcortical infarction. Journal of Cerebral Blood Flow and Metabolism 2014; 34: 597–605. DOI: 10.1038/jcbfm.2013.238.

Insights of Clinical and Medical Images

34. Ralph MAL. Measuring language recovery in the underlying large-scale neural network: Pulling together in the face of adversity. Annals of Neurology 2010; 68: 570–572. DOI: 10.1002/ana.22213.
35. Crone EA, Wendelken C, Donohue SE, et al. Neural evidence for dissociable components of task-switching. Cerebral Cortex 2006; 16: 475–486. DOI: 10.1093/cercor/bhi127.
36. Menon V. Large-scale brain networks and psychopathology: a unifying triple network model. Trends in Cognitive Sciences 2011; 15: 483–506. DOI: 10.1016/j.tics.2011.08.003.
37. Gürsel DA, Reinholz L, Bremer B, et al. Frontoparietal and salience network alterations in obsessive–compulsive disorder: insights from independent component and sliding time window analyses. Journal of Psychiatry & Neuroscience 2020; 45: 214–221. DOI: 10.1503/jpn.190038.
38. Seeley WW, Menon V, Schatzberg AF, et al. Dissociable intrinsic connectivity networks for salience processing and executive control. The Journal of Neuroscience 2007; 27: 2349–2356. 2007/03/03. DOI: 10.1523/jneurosci.5587-06.2007.
39. Dodds CM, Morein-Zamir S and Robbins TW. Dissociating inhibition, attention, and response control in the frontoparietal network using functional magnetic resonance imaging. Cerebral Cortex 2011; 21: 1155–1165. DOI: 10.1093/cercor/bhq187.